EARTHQUAKE ENGINEERING AND STRUCTURAL DYNAMICS, VOL. 25, 927-944 (1996)

CONVEX MODEL FOR SEISMIC DESIGN OF STRUCTURES—I: ANALYSIS

C. P. PANTELIDES* AND S.-R. TZAN†

Department of Civil Engineering, 3220 Merrill Engineering Building, University of Utah, Salt Lake City, UT 84112, U.S.A.

SUMMARY

A convex model is used to estimate the maximum response of structural systems subjected to uncertain seismic excitations. The convex modal is based on the assumption that the energy of the excitation is bounded . A reduction factor, defined in the modal domain by dividing the results obtained from the convex model by those from the time history of the actual record, is used to calibrate the convex model. An average reduction factor is also defined by averaging a set of excitation-specific reduction factors. The average reduction factor can be used for unknown excitations with an assumed energy bound and certain common earthquake characteristics. These common characteristics can be defined either by a set of previous earthquakes in the region or by regional earthquake spectra. The convex model using the average reduction factor yields acceptable predictions of the maximum response.

KEY WORDS: convex model; global energy bound; reduction factor; seismic excitation; spectrum; structures

INTRODUCTION

Various researchers have developed methods which estimate the maximum response of structural systems to earthquake excitations. Drenick[1,2] proposed the idea that highly variable but limited deterministic information characterizing the ground motion could be used to find the least favourable response of a structural system to an earthquake. The total energy which the earthquake is likely to develop at the structure's location was used; a 'critical excitation' was sought within the set of allowable dynamic forces which maximizes the structural response. However, since only total energy had to be bounded, the result was rather conservative. Shinozuka[3] has suggested characterizing the earthquake excitation by specifying an envelope of the Fourier amplitude spectrum. This measure yields much less conservative results than Drenick's since the information embodied in the measure constrains the set of possible excitations considerably; as a result the maximum structural response magnitude is reduced. Several Liapunov bounds on the maximum response of elastic structures subjected to combined horizontal and vertical earthquake ground motions were obtained by Ahmadi.[4] However, the method requires knowledge of appropriate effective time duration of maximum ground accelerations to yield reasonable results. In addition to the above methods for estimating the maximum structural response in an earthquake, statistical methods[5-7] as well as probabilistic methods[8,9] have been proposed.

Ground motions involve large variability due to source effects associated with the rupture process, path effects related to wave propagation between a source and a site, and site effects due to soil conditions and topography.[10] The magnitude, intensity, duration, envelope of the amplitude spectrum, and epicentral distance of an earthquake are uncertain parameters that are usually unavailable for design and make the task of estimating the maximum structural response very difficult. A recent study of a large database containing 1500 records of earthquake ground motion has shown that instead of using elastic and inelastic spectra for

*Associate Professor
†Research Assistant

CCC 0098-8847/96/090927-18

Received 6 February 1995
Revised 5 October 1995

design, which do not contain the effect of strong motion duration, it may be more realistic to use input and hysteretic energy spectra.[11]

Recently, Ben-Haim and Elishakoff[12] used convex models to represent uncertain dynamic excitations. Convex models provide a non-probabilistic representation of uncertainty. They are especially applicable when only a limited amount of information is available, as in the case of earthquake excitations. In the convex model approach, the uncertainty in the excitation is usually represented as a bound on the Fourier coefficients of the expansion of the excitation,[13–18] as a bound on the energy of the excitation,[18,19] or an envelope function with upper and lower limits.[12,18] The concept of convex modelling and its relationship with the theory of probability and fuzzy sets was described by Elishakoff.[20] A convex model of the base acceleration in terms of an upper bound was used along with linear programming to obtain the least favourable structural response.

In this paper, a convex model is used to estimate the maximum response of single-degree-of-freedom and multiple-degree-of-freedom structural systems which are subjected to uncertain future earthquakes with known energy bound and certain common site characteristics. These common site characteristics can be obtained from either previous earthquakes in the region or from regional earthquake spectra.

GLOBAL ENERGY-BOUND CONVEX MODEL (GEB)

A convex model is a method of quantifying uncertainty, in this case the uncertain nature of earthquakes, without resorting to probabilistic concepts; instead, the uncertainty is characterized by a set of functions with common global characteristics.[12,18] The application of convex models to represent uncertainty is well suited in situations where only a limited amount of information is available, which is exactly the case for structural systems subjected to uncertain excitations such as earthquakes. The convex model constrains the uncertainty, inherent in earthquake excitations, within a bound which is defined in terms of a function of bounded energy of the earthquake. In this paper, the global energy-bound convex model is considered.

The equation of motion for a multiple-degree-of-freedom (MDOF) structure is used in its normalized form with respect to the mass matrix. Let the natural frequencies of the structure be $\omega_1, \ldots, \omega_N$, the corresponding mode shapes be $\phi_1, \ldots, \phi_N$, and the corresponding modal matrix be $\Phi = [\phi_1, \ldots, \phi_i, \ldots, \phi_N]$, where N is the number of modes. The normalized properties with respect to the mass matrix can be expressed as

$$\Phi^{\mathrm{T}}\mathbf{M}\Phi = \mathrm{I}; \qquad \Phi^{\mathrm{T}}\mathbf{K}\Phi = \begin{bmatrix} \omega_1^2 & & & \mathrm{O} \\ & \ddots & & \\ & & \omega_i^2 & \\ & & & \ddots \\ \mathrm{O} & & & \omega_N^2 \end{bmatrix}$$

$$\Phi^{\mathrm{T}}\mathbf{C}\Phi = \begin{bmatrix} 2\omega_1\xi_1 & & & \mathrm{O} \\ & \ddots & & \\ & & 2\omega_i\xi_i & \\ & & & \ddots \\ \mathrm{O} & & & 2\omega_N\xi_N \end{bmatrix} \tag{1a}$$

where $\mathbf{I}$ is an $N \times N$ identity matrix, and ξ_i is the ith mode damping ratio of the structure; the equation of motion can be expressed for each mode as

$$\ddot{y}_i + 2\xi_i\omega_i\dot{y}_i + \omega_i^2 y_i = \phi_i^{\mathrm{T}}\Theta\ddot{X}_g(t) \tag{1b}$$

where $y_i(t)$ is the ith mode displacement response in normal co-ordinates, Θ is a vector of ones and $\ddot{X}_g(t)$ is the horizontal ground acceleration.

Using Duhamel's integral and assuming zero initial conditions, the response of the structure in the ith normal mode is

$$y_i(t) = \frac{1}{\omega_{D,i}} \int_0^t \phi_i^T \Theta \ddot{X}_g(\tau) e^{-\xi_i \omega_i (t-\tau)} \sin \omega_{D,i}(t-\tau)\, d\tau, \quad i = 1, \ldots, N \tag{2a}$$

$$\omega_{D,i} = \omega_i \zeta_i, \quad \zeta_i = \sqrt{1-(\xi_i)^2} \tag{2b}$$

The ith modal velocity and acceleration in normal co-ordinates for zero initial conditions are given in the appendix. The displacement, velocity and acceleration in physical co-ordinates are then obtained from the following superposition equations:

$$\mathbf{x}(t) = \Phi \mathbf{y}(t); \quad \dot{\mathbf{x}}(t) = \Phi \dot{\mathbf{y}}(t); \quad \ddot{\mathbf{x}}(t) = \Phi \ddot{\mathbf{y}}(t) \tag{3}$$

In what follows, the ground acceleration, $\ddot{X}_g(t)$, is assumed to belong to a convex set bounded by a global energy-bound model.

The values of the displacement, velocity, and acceleration are evaluated based on the convex set of admissible ground accelerations. For the global energy bound (GEB) convex model, this set can be expressed as[12]

$$S_{GEB} = \left\{ \ddot{X}_g(t): \int_0^t [\ddot{X}_g(\tau)]^2 \, d\tau \leqslant E_{GEB}^2(t) \right\} \tag{4}$$

The global energy bound, $E_{GEB}^2(t)$, varies with time; however, as time goes to infinity the bound reaches a finite value $E_{GEB}^2(\infty)$ which is larger than any $E_{GEB}^2(t)$. Note that time is equal to infinity at the end of the earthquake duration, i.e. $t_\infty = t_f$, where t_f is the earthquake duration. The peak values of modal displacement, velocity and acceleration can be found using the theory of convex models.[12] Let the peak value of the displacement of the ith normal mode for the GEB convex model be $y_{GEB,i}$. This value and the corresponding values for the ith normal mode velocity and acceleration can be obtained as shown in the appendix; the values as time goes to infinity are given by taking the limit of equations (14)–(16), which yield

$$y_{GEB,i} = \frac{\phi_i^T \Theta E_{GEB}(\infty)}{2\omega_i \sqrt{\xi_i \omega_i}} \tag{5a}$$

$$\dot{y}_{GEB,i} = \frac{\phi_i^T \Theta E_{GEB}(\infty)}{2\sqrt{\xi_i \omega_i}} \tag{5b}$$

$$\ddot{y}_{GEB,i} = \frac{\phi_i^T \Theta E_{GEB}(\infty)}{2} \sqrt{\frac{\omega_i [1 + 4(\xi_i)^2]}{\xi_i}} \tag{5c}$$

The quantity $E_{GEB}^2(\infty)$ is defined as shown in equation (4) with $t_\infty = t_f$. Equation (5) shows that the only quantity required to obtain the convex model estimate of the response, in addition to the damping, frequency, and mode shape, is the global energy bound of the earthquake evaluated at the end of the earthquake record. The maximum response in physical co-ordinates can be approximated by the square root of the sum of the squares (SRSS) of the modal responses as

$$|x_{max,j}| \cong \sqrt{\sum_{i=1}^{N} \phi_{ji}^2 y_{GEB,i}^2}, \quad |\dot{x}_{max,j}| \cong \sqrt{\sum_{i=1}^{N} \phi_{ji}^2 \dot{y}_{GEB,i}^2}, \quad |\ddot{x}_{max,j}| \cong \sqrt{\sum_{i=1}^{N} \phi_{ji}^2 \ddot{y}_{GEB,i}^2} \tag{6}$$

The subscript j denotes the response at the jth degree of freedom and i denotes the ith mode; N is the number of dynamic modes of the system. However, when the SRSS method is used, only the significant modes need to be considered. When major contributing modes have frequencies that are close together, the complete quadratic combination (CQC) method should be used.[21]

Example 1—Convex model and reduction factor for a single-degree-of-freedom structural system

Consider a single-degree-of-freedom (SDOF) structural system subjected to the S00E record of the 18 May 1940 El-Centro earthquake which is shown in Figure 1. The displacement responses obtained by: (1) a time-history analysis employing the actual record (AR), and (2) the global energy-bound convex model (GEB) are shown in Figure 2. The fundamental period of the structure is 1·0 sec and the damping level is 5 per cent of critical. The maximum response obtained by the AR analysis is 0·13 m and that by the GEB analysis is 0·48 m. The time-history displacement for the structure with a damping level of 10 per cent of critical is shown in Figure 3. The maximum response obtained by the AR analysis is 0·09 m and that by the GEB

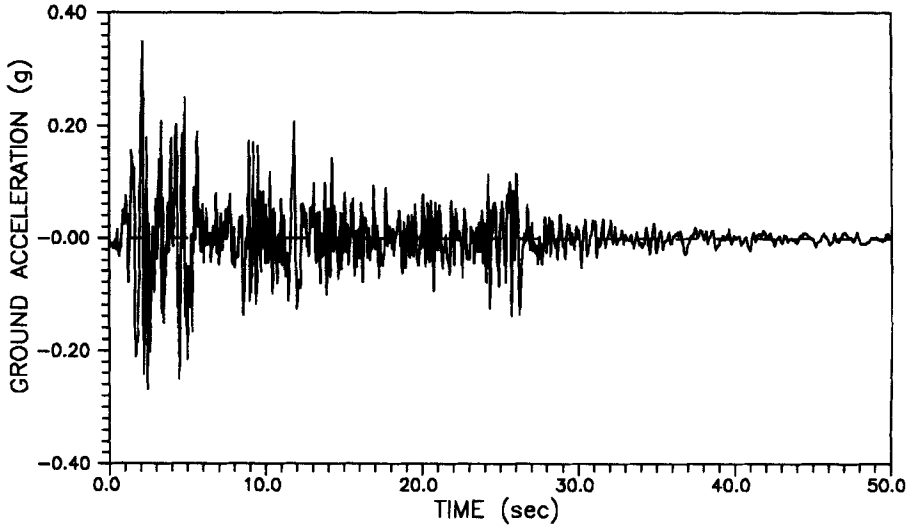

Figure 1. The S00E record of the May 18, 1940 El-Centro (Imperial Valley, CA) earthquake

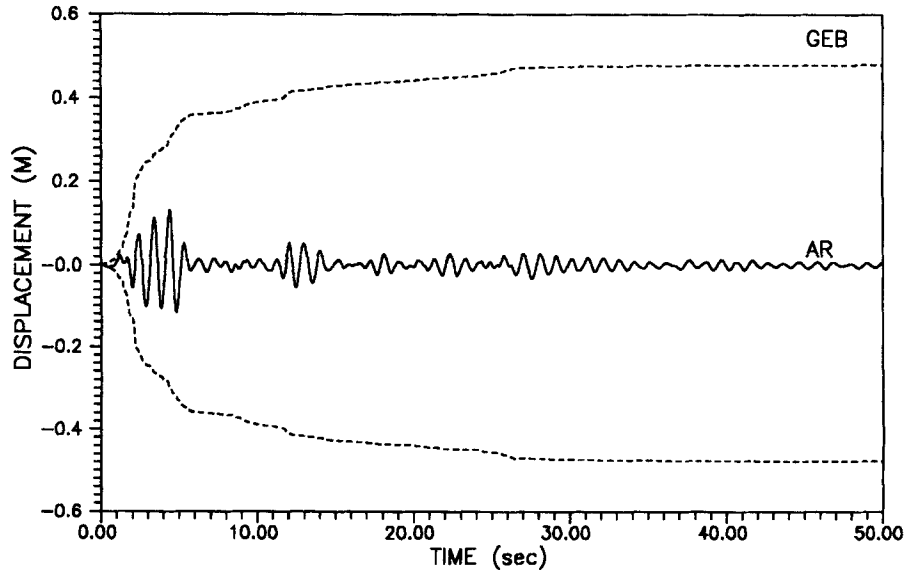

Figure 2. Displacement time-history of a SDOF system with damping level of 5 per cent of critical for the 1940 El-Centro earthquake: (———) actual record (AR); (– – –) global energy-bound convex model (GEB)

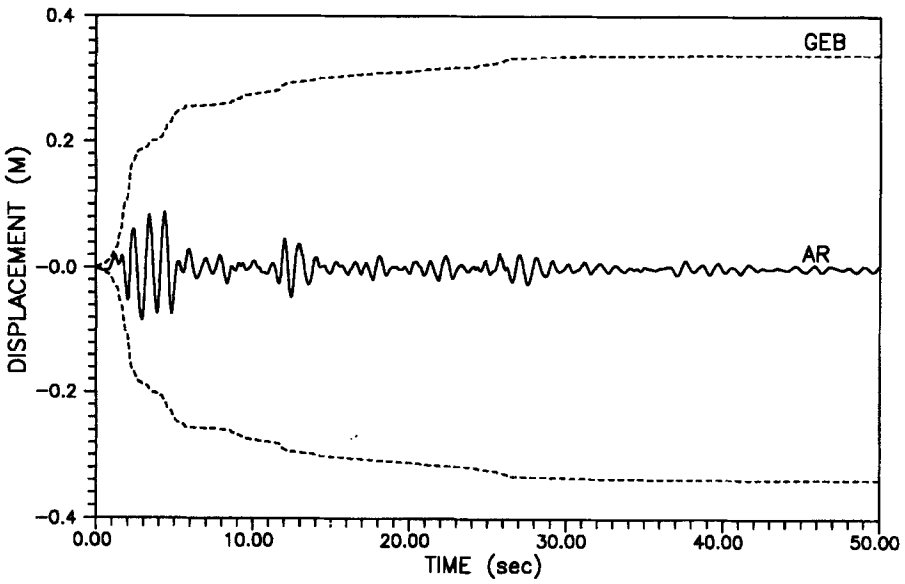

Figure 3. Displacement time-history of a SDOF system with damping level of 10 per cent of critical for the 1940 El-Centro earthquake: (———) actual record (AR); (– – –) global energy-bound convex model (GEB)

analysis is 0·34 m. It can be observed that the convex model gives bounds that are relatively closer to the actual maxima for higher levels of damping. This property is desirable in the design of active structures, which inherently have high levels of damping.[22]

For the case with a damping level of 5 per cent of critical, the response obtained by the global energy-bound (GEB) convex model gives a higher value than the maximum response evaluated using a time-history analysis of the actual record (AR) by a ratio, $(GEB/AR)_d = 3{\cdot}71$ for the maximum displacement, $(GEB/AR)_v = 3{\cdot}30$ for the maximum velocity, and $(GEB/AR)_a = 2{\cdot}80$ for the maximum acceleration. This suggests that a reduction factor could be used to reduce the conservatism of the results obtained by the convex model for the maximum displacement, velocity, and acceleration response.

In general, the reduction factor for a given excitation is a function of the period and the damping ratio of the SDOF structure. Figure 4 shows the reduction factors for the displacement and velocity response obtained by using the GEB convex model for the 1940 El-Centro earthquake. Figure 4(a) was obtained by the convex model of equations (5a) and (2) using a time-history analysis of the actual record (AR) for a damping level of 2, 6, and 10 per cent of critical. The reduction factor for the GEB model for displacement is obtained by dividing the result of equation (5a) by the maximum actual response obtained from equation (2) for a given period and damping ratio. A similar procedure is used to define the reduction factor for velocity and acceleration by using equations (5b) and (7) in the appendix and equations (5c) and (8), respectively. It can be observed that for higher levels of damping the reduction factor is reduced. These figures can be used to estimate the expected maximum response to an earthquake for either SDOF or multiple-degree-of-freedom (MDOF) structural systems as shown in the next section.

GLOBAL ENERGY-BOUND CONVEX MODEL ADJUSTED WITH AN EXCITATION-SPECIFIC REDUCTION FACTOR (RGEB)

For a given earthquake record, the reduction factor can be obtained from the period and damping ratio for each mode of the structure. A simple method for calculating the reduction factor is to create a database as a function of period and damping ratio. An interpolation technique can be used to find the value of the reduction factor between two intervals of period and two intervals of damping. A calibration curve which is a function of the period and damping ratio of the structure can be created for the best fit to the given database.[23]

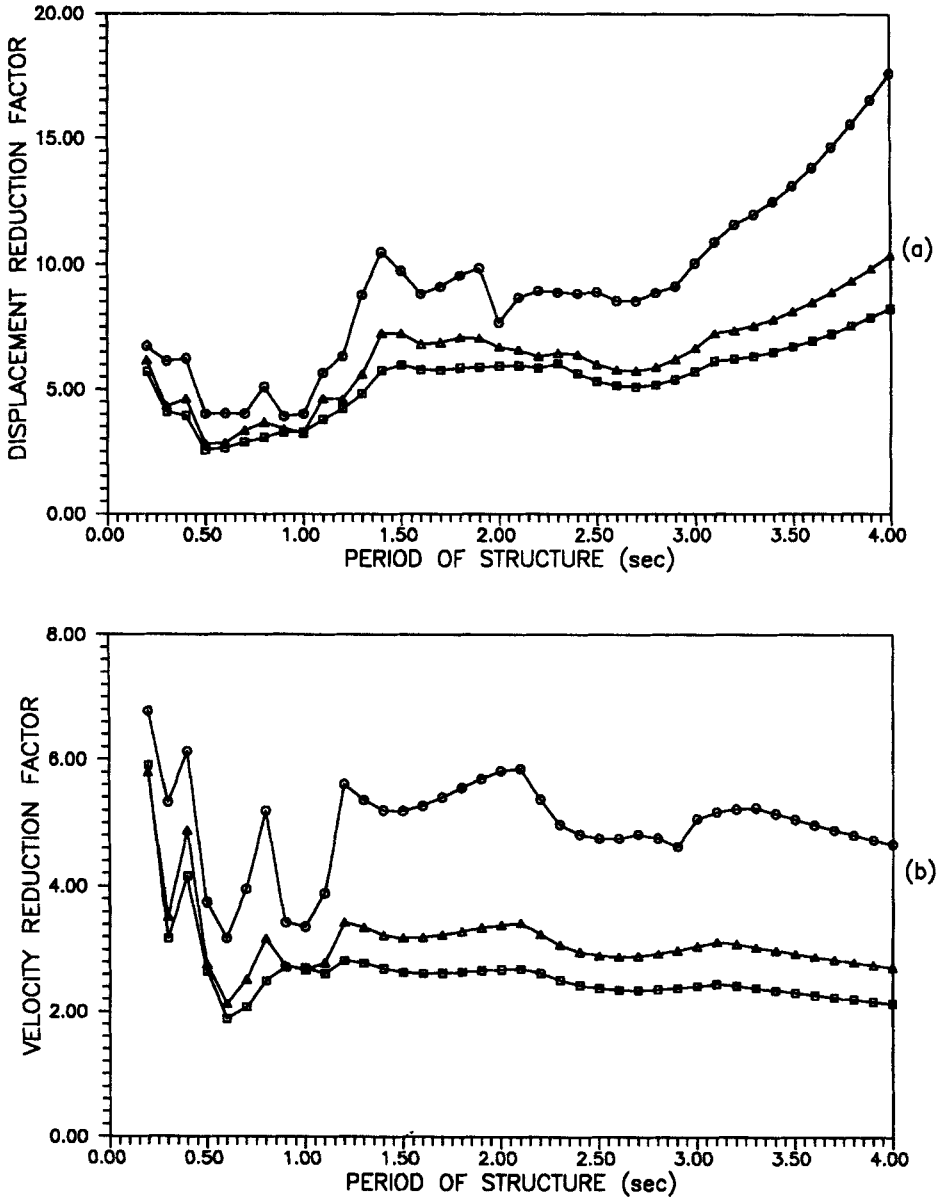

Figure 4. Global energy-bound reduction factor for the 1940 El-Centro earthquake (a) displacement and (b) velocity: (—⊖—) damping level of 2 per cent of critical; (—△—) damping ratio of 6 per cent of critical; (—⊟—) damping ratio of 10 per cent of critical

The procedure for determining the displacement response using the excitation-specific reduction factors is as follows: once the reduction factor for each mode is found, the modal response obtained from the GEB convex model of equation (5) is divided by the respective reduction factor. Subsequently, the physical response is obtained by the square root of the sum of the squares (SRSS) of the adjusted modal responses (equation (6)). Similar procedures are adopted for finding the velocity and acceleration.

The model described above is defined as the RGEB and model (global energy-bound convex model adjusted with an excitation-specific reduction factor). Note that the reduction factors defined above depend on the properties of the particular earthquake under consideration (here for El-Centro, 1940 as shown in Figure 4), and will be different for other earthquakes. The usefulness of the RGEB convex model is limited to

evaluating the maximum structural response for a given earthquake, but for structures with different properties of natural periods and damping. In addition, the RGEB convex model is useful in the definition of a more general convex model which can predict the maximum structural response for uncertain earthquakes with certain common characteristics, as will be shown in the next section.

Example 2—Maximum response of ten-storey frame subjected to earthquake records

The ten-storey frame of Figure 5 is used to test the RGEB convex model. The cross-sectional areas and second moments of area of the beams and columns of the frame are shown in Table I. The structural frequencies of the ten-storey frame are 4·07, 12·09, 22·25, 34·29, 48·11, 63·92, 81·33, 97·25, 113·79, 129·22 rad/sec. The damping level is assumed to be 5 per cent of critical for all modes and only one horizontal degree-of-freedom is considered per floor. Table II shows the maximum response obtained by (1) using the time history (equation (3)) of the actual record (AR), (2) the GEB convex model, and (3) the RGEB convex model. The 1940 El-Centro earthquake of Figure 1 is used. The response ratios for the GEB and RGEB models with respect to the actual record (AR) analysis are also shown in Table II. It can be observed that the displacement, velocity, and acceleration response obtained by the GEB convex model is on average 8·2, 6·5, and 3·7 times larger, respectively, than that obtained using the actual record from equation (3). The differences in the displacement, velocity, and acceleration response obtained by the RGEB convex model and the actual record (AR) analysis are within 27, 39, and 42 per cent. On average, the results obtained by the

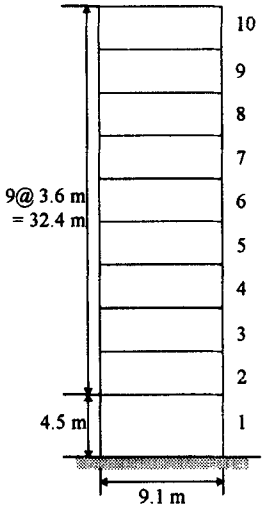

Figure 5. Ten-storey frame for Examples 2, 3, and 4

Table I. Member sizes for ten-storey frame

	Beam		Column	
Floor	Area ($\times 10^{-2}$ m^2)	Second moment of area ($\times 10^{-4}$ m^4)	Area ($\times 10^{-2}$ m^2)	Second moment of area ($\times 10^{-4}$ m^4)
1	4·02	18·65	4·66	25·03
2–4	3·69	15·69	4·41	22·51
5–7	3·63	15·25	4·15	19·90
8–10	3·17	11·59	3·48	13·96

Table II. Maximum response of the ten-storey frame for the 1940 El-Centro earthquake record

Floor	AR	GEB	GEB/AR	RGEB	RGEB/AR
Displacement (cm)					
1	1·37	11·14	8·13	1·74	1·27
2	3·18	26·25	8·25	3·98	1·25
3	5·09	42·79	8·41	6·23	1·22
4	6·89	59·05	8·57	8·23	1·19
5	8·78	74·60	8·50	9·95	1·13
6	10·71	88·77	8·29	11·45	1·07
7	12·57	101·31	8·06	12·84	1·02
8	14·34	112·81	7·87	14·30	1·00
9	15·79	122·15	7·74	15·68	0·99
10	16·84	128·66	7·64	16·75	0·99
Velocity (cm/sec)					
1	10·70	63·25	5·91	14·83	1·39
2	22·49	129·61	5·76	30·14	1·34
3	32·96	193·89	5·88	42·85	1·30
4	41·58	253·29	6·09	50·75	1·22
5	49·73	308·43	6·20	54·21	1·09
6	55·68	358·59	6·44	55·31	0·99
7	59·19	404·31	6·83	57·10	0·96
8	58·61	448·69	7·66	63·03	1·08
9	67·49	488·95	7·24	73·34	1·09
10	77·19	522·41	6·77	83·69	1·08
Acceleration (cm/sec^2)					
1	348·59	1584·31	4·54	495·11	1·42
2	541·52	1722·54	3·27	624·28	1·15
3	636·71	1886·39	2·96	734·39	1·15
4	568·89	1973·75	4·47	791·51	1·39
5	576·92	2062·58	3·58	762·08	1·32
6	516·60	2128·05	4·12	733·23	1·42
7	540·96	2236·70	4·13	662·69	1·23
8	576·64	2349·90	4·08	704·30	1·22
9	709·31	2495·88	3·52	827·42	1·17
10	923·82	2876·45	3·11	978·98	1·06

RGEB convex model are 11·3, 15·4 and 25·3 per cent larger than the response using a time history of the actual record for the displacement, velocity, and acceleration. The improvement in the prediction of the maximum response using the RGEB convex model is obvious compared to the GEB convex model.

GLOBAL ENERGY-BOUND CONVEX MODEL USING AVERAGE REDUCTION FACTOR (ARGEB)

The results obtained by the RGEB convex model are less conservative than those obtained by the GEB convex model, and the maximum response is within reasonable agreement compared to the actual results from a time history of the earthquake record. However, the reduction factor obtained by the RGEB convex model can only be used for a given earthquake excitation, which is not known before it occurs. It should be noted that the reduction factors are independent of the absolute value of the global energy bound.

In order to extend the results obtained by the RGEB convex model to other unknown earthquakes, it is necessary to have additional information besides the value of the global energy bound. This is necessary because of the variations in frequency content of earthquakes originating at different locations, variations due to soil conditions, topography and others. For an uncertain excitation, which may be different from the 1940 El-Centro earthquake considered so far, an average reduction factor of the global energy-bound convex

model (ARGEB) is defined by using one of two methods: (1) collect a set of actual past earthquake records in the vicinity of the site and average the RGEB reduction factors of the set, or (2) construct a set of artificial earthquake records from a known spectrum in the proximity of the site and average the RGEB reduction factors of the set. For the RGEB convex model the reduction factor was obtained as described in the previous section. For the ARGEB convex model, the average reduction factor for each subset is obtained by averaging the earthquake-specific reduction factors (RGEBs) for all the earthquake records in the subset. Subsequently, the response obtained from equation (5) must be divided by the average reduction factor for each mode (ARGEB), and the final response is obtained using equation (6).

Example 3—Maximum response of ten-storey frame subjected to past earthquake records

Thirty-two past earthquake records described in Table III are used to evaluate the performance of the ARGEB convex model. Table IV shows the eight subsets of the above records defined for the purpose of this

Table III. Earthquake records used to investigate the ARGEB convex model

No.	Earthquake	Date	Location	Component	Peak accel. (g)
Earthquakes in California (U.S.)					
1	El-Centro	18 May 1940	Imperial Valley	S00E	0·348
2				S90W	0·214
3	Taft	21 July 1952	Kern county (Taft Lincoln school)	S69E	0·179
4				N21E	0·156
5	San Fernando	9 February 1971	Pacoima Dam	S16E	1·172
6				1·076	1·076
7	Loma Prieta	17 October 1989	Oakland-outer harbour wharf-channel 1	270°	0·276
8			Channel 3	0°	0·220
9			Channel 4	270°	0·276
10			Channel 5	270°	0·298
11			Channel 6	270°	0·305
12			Channel 7	0°	0·277
13			Channel 8	0°	0·436
14			Channel 9	270°	0·296
15			Channel 10	270°	0·269
16			Channel 12	0°	0·287
17	Northridge	17 January 1994	Santa Monica—City Hall	90°	0·885
18				0°	0·370
19			Sylmar—County hospital	0°	0·844
20				90°	0·605
21			Newhall—LA County fire station	0°	0·590
22				90°	0·583
23			Pacoima Dam—Downstream	0°	0·434
24				175°	0·415
25			Arleta—Nordoff Ave. fire station	90°	0·344
26				0°	0·308
Earthquakes in Mexico					
27	Mexico City	19 September 1985	Coast of Buerrero-Michoacan	N90W	0·171
28				S00E	0·100
Earthquakes in Japan					
29	Hachinohe	May 1968	—	S-N	0·228
30				E-W	0·180
31	Miyagi	12 June 1978	—	S-N	0·263
32				E-W	0·205

Table IV. Subsets of earthquake records used in the ARGEB convex model

Subset	Description	Record (see Table III)
S1	El-Centro, 18 May 1940	1, 2
S2	San Fernando, 9 February 1971	5, 6
S3	Loma Prieta, 17 October 1989	7–16
S4	Northridge, 17 January 1994	17–26
S5	El-Centro, 18 May 1940 and Taft, 21 July 1952	1–4
S6	San Fernando, 9 February 1971 and Northridge, 17 January 1994	5, 6, 17–26
S7	California records	1–26
S8	California, Mexico City, 19 September '85, Hachinohe, May '68, and Miyagi, 12 June '78	1–32

Table V. Response ratio for maximum response using the RGEB and the ARGEB convex models for past earthquake records

	Max. displacement	Max. velocity	Max. acceleration
1940 El-Centro earthquake (S00E)-AR1			
RGEB/AR1	1·11	1·15	1·25
ARGEB(S1)/AR1	1·07	1·21	1·00
ARGEB(S5)/AR1	1·14	1·10	0·94
ARGEB(S7)/AR1	1·61	1·48	1·14
ARGEB(S8)/AR1	1·56	1·33	0·81
1971 San Fernando earthquake (S16E)-AR2			
RGEB/AR2	1·03	0·94	1·30
ARGEB(S2)/AR2	0·74	0·79	1·26
ARGEB(S4)/AR2	0·79	0·82	1·22
ARGEB(S6)/AR2	0·78	0·81	1·21
ARGEB(S7)/AR2	0·87	0·86	1·05
ARGEB(S8)/AR2	0·85	0·77	0·74
1989 Loma Prieta earthquake-Oakland-outer harbour wharf (channel 8)-AR3			
RGEB/AR3	0·96	0·90	1·20
ARGEB(S3)/AR3	1·27	1·07	0·95
ARGEB(S7)/AR3	0·87	0·80	0·96
ARGEB(S8)/AR3	0·85	0·72	0·67
1994 Northridge earthquake-Santa Monica City Hall (S90N)-AR4			
RGEB/AR4	1·04	1·24	1·96
ARGEB(S2)/AR4	1·00	1·22	1·16
ARGEB(S4)/AR4	1·07	1·27	1·12
ARGEB(S6)/AR4	1·06	1·25	1·12
ARGEB(S7)/AR4	1·18	1·33	0·97
ARGEB(S8)/AR4	1·15	1·19	0·71

study. A response ratio is defined in the present example by dividing the response obtained using the convex model by the response obtained using the time-history of the actual record. This ratio is averaged over all floors and is shown in Table V for both the RGEB and ARGEB convex models.

It can be observed that the response ratio for the results obtained by the RGEB convex model is within 30 per cent for all four records, except for the acceleration in the Northridge earthquake (96 per cent). The response ratio for the results obtained by the ARGEB convex model for the eight subsets defined in Table IV, indicates acceptable predictions of the maximum response. As expected, the RGEB convex model yields in general better results than the ARGEB model. For all four actual records in Table V, the accuracy of the

prediction of the response progressively decreases as more earthquakes are added from different locations, i.e. compare (S7) to (S8). Hence, the reduction factors are sensitive with respect to the location of the subset of earthquakes used to determine the average reduction factor for each mode. However, the results obtained for the 1971 San Fernando actual earthquake (S16E) using subsets (S2), (S4), and (S6) are close. Similarly, the results obtained for the 1994 Northridge actual earthquake (Santa Monica City Hall, S90N) using subsets (S2), (S4), and (S6) are also close. This shows that the average reduction factors at approximately the same general location are not very sensitive to time.

Example 4—Maximum response of ten-storey frame subjected to artificial earthquakes

The ten-storey frame described in Example 2 is used to investigate the performance of the RGEB and ARGEB convex models subjected to several artificial earthquakes. Three groups of artificial earthquakes are generated by the SIMQKE program.[24] The spectrum of the first group (G1) is chosen from the example spectrum of the SIMQKE program to create six artificial earthquakes shown in Figure 6. All records have a peak acceleration of 0·5 g and a duration of 50 s. However, the global energy bound is not the same; as noted earlier, this fact does not change the values of the reduction factors. Note also that even though the global energy bound is different for the artificial earthquakes, this does not affect the results which are expressed in dimensionless form. The six artificial earthquakes shown in Figure 7 are included in the second group (G2) which are created by the spectrum developed by Housner.[6] The spectrum of Figure 8(a) was constructed from the average response of fifteen earthquakes.[25] This spectrum was used to create the third group of six artificial earthquakes (G3) as shown in Figures 8(b)–8(g). The fourth group (G4) considers the set defined by G1, G2, and G3 together (see Table VI). The average reduction factors are then determined independently for each group of artificial earthquakes stated above.

Table VII shows the response ratio of the RGEB and ARGEB convex models to the time-history analysis of the actual record (AR) for the following artificial earthquakes: 6(c), 6(f), 7(b), 7(d), 8(b), and 8(g). The response ratio for the results obtained by the RGEB convex model is within 10 and 13 per cent for the displacement and velocity, and 93 per cent for the acceleration. In general, the response ratios of the ARGEB convex model compared with the actual record (AR) are larger than the ratios of the RGEB convex model. However, the response ratio for the results obtained by the ARGEB convex model still yields acceptable predictions of the response for the artificial earthquakes.

The ARGEB convex model of Group 2(see Table VI) is used to predict the response for an unknown future excitation which has a known site spectrum and energy bound. An artificial earthquake which is shown in Figure 9 was created by using the spectrum of Figure 7(a), and is used to examine the validity of the results. The estimated displacement and velocity obtained by the ARGEB model for Group 2 and the time history of the actual record are shown in Figure 10. It can be observed that the predicted results are slightly underestimated, but the difference between the ARGEB model and the actual record is still within 10 per cent for both the displacement and velocity response.

CONCLUSIONS

The estimated structural response using the energy-bound convex model is rather conservative when compared to the time history of the response using the actual earthquake record. The energy-bound convex model results are slightly improved as the damping level of the structure is increased. A reduction factor is defined for a structure subjected to a specific earthquake record and is a function of the structure's natural periods and modal damping ratios (RGEB convex model).

The results are extended for finding the maximum response of a structure to an unknown excitation but known energy bound. An average reduction factor is defined by taking the average of the reduction factors from a set of earthquake records. Numerical simulations show that the response obtained by the global energy-bound model adjusted by the average reduction factor (ARGEB convex model) is different from the response obtained by the excitation-specific RGEB model. However, the ARGEB model still yields an

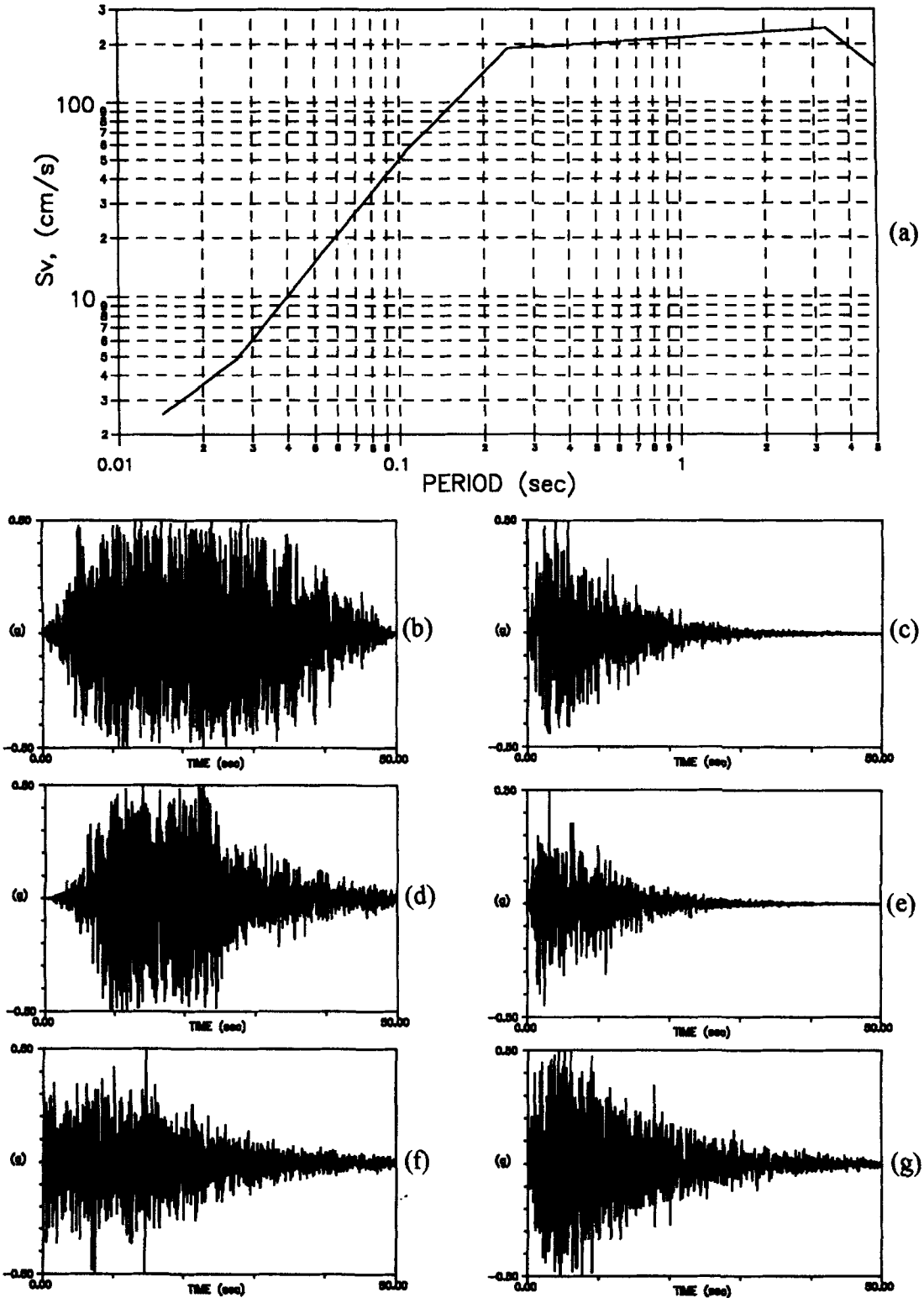

Figure 6. Artificial earthquakes of Group 1: (a) spectrum; (b)–(g) artificial earthquakes

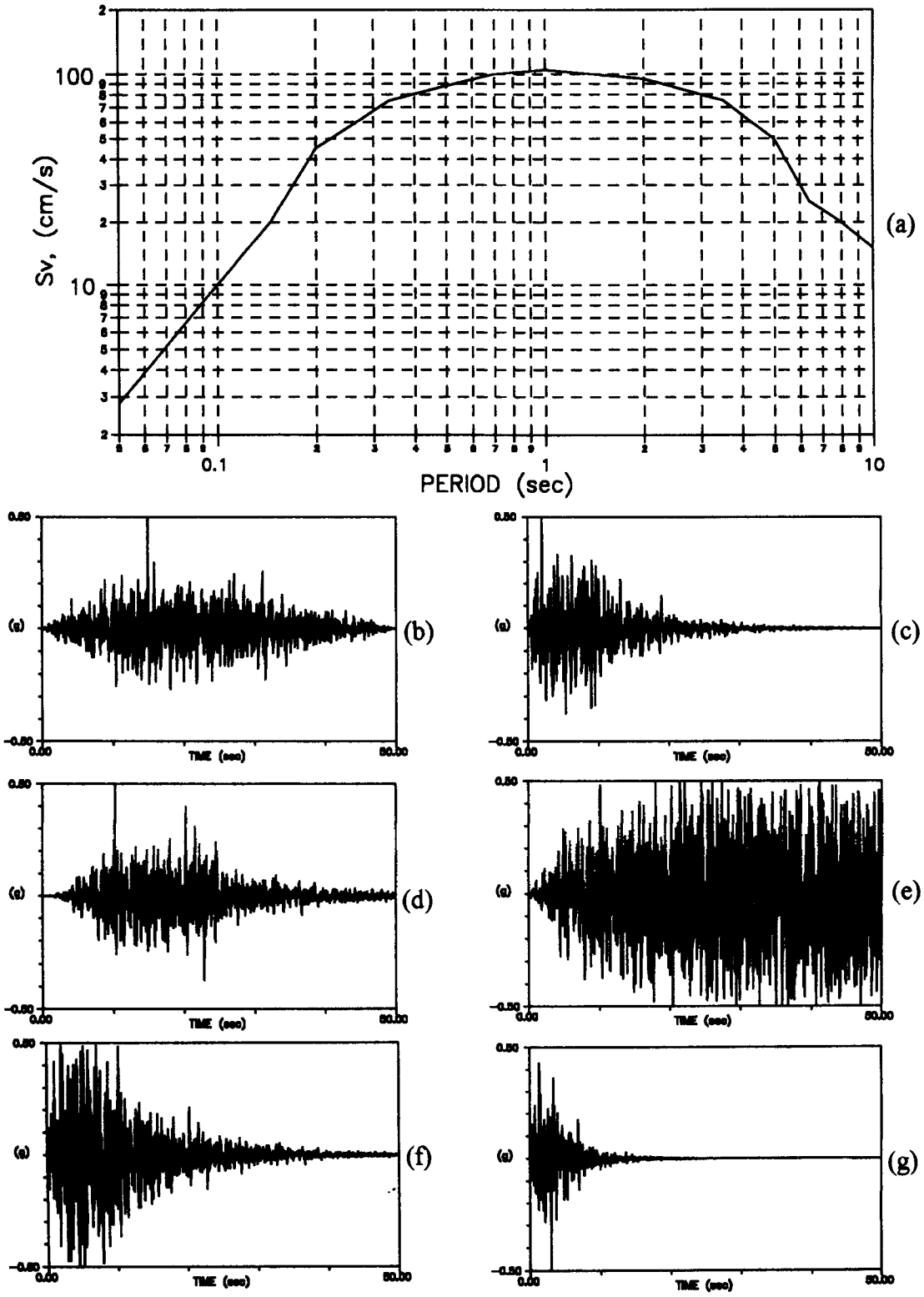

Figure 7. Artificial earthquakes of Group 2: (a) spectrum; (b)–(g) artificial earthquakes

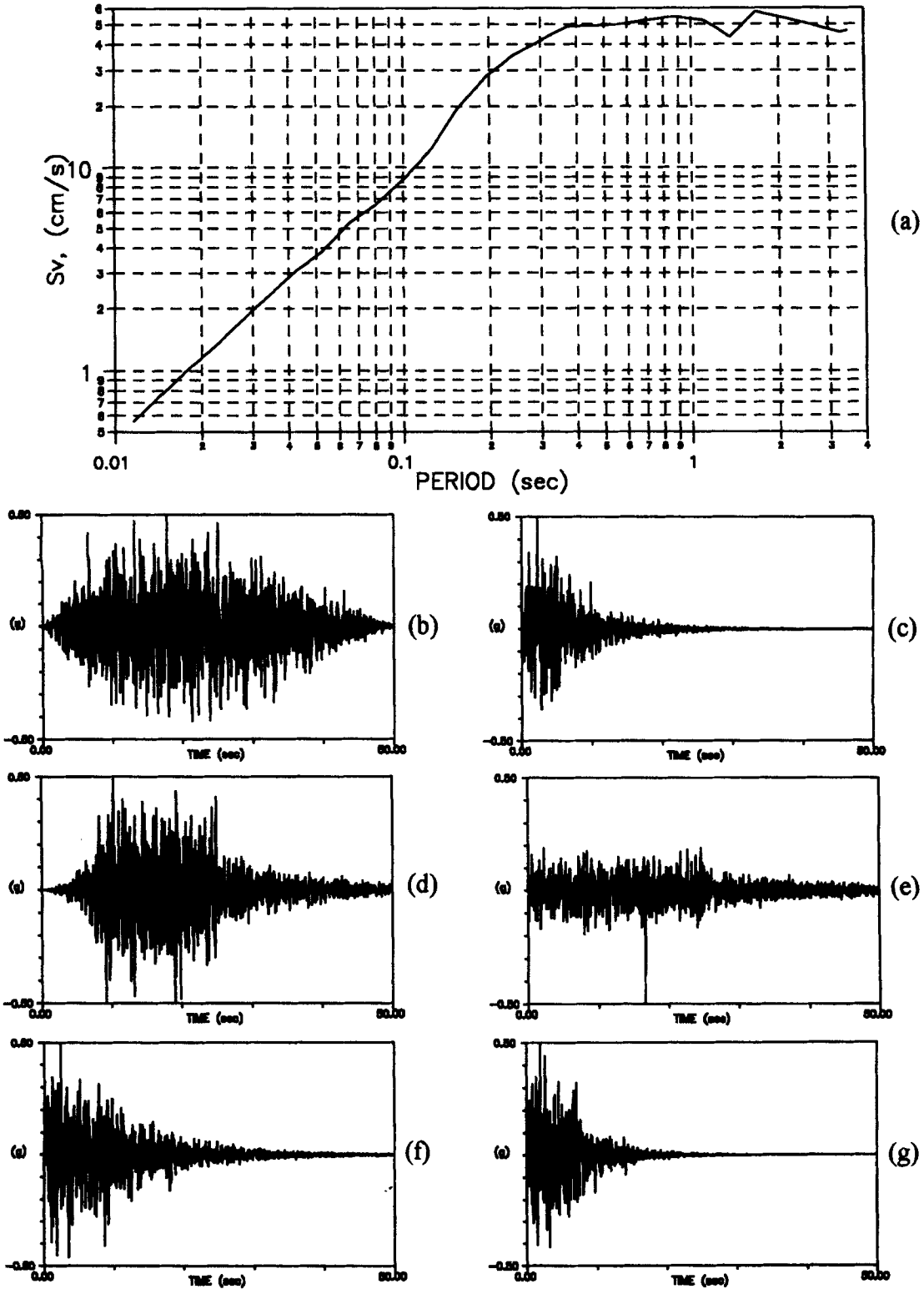

Figure 8. Artificial earthquakes of Group 3: (a) spectrum; (b)–(g) artificial earthquakes

Table VI. Groups of artificial earthquakes used in the ARGEB convex model

Group	Description	Earthquake records
G1	Created by spectrum shown in Figure 6(a)	Figures 6(b)–6(g)
G2	Created by spectrum shown in Figure 7(a)	Figures 7(b)–7(g)
G3	Created by spectrum shown in Figure 8(a)	Figures 8(b)–8(g)
G4	Includes Groups 1, 2, and 3	Figures 6(b)–6(g), 7(b)–7(g), and 8(b)–8(g)

Table VII. Response ratio for maximum response using the RGEB and the ARGEB convex models for artificial earthquakes

Response	Max. displacement	Max. velocity	Max. acceleration
Artificial earthquake in Group 1 (Figure 6(c))-AR6(c)			
RGEB/AR6(c)	1·06	1·09	1·86
ARGEB(G1)/AR6(c)	1·21	1·00	1·11
ARGEB(G4)/AR6(c)	1·53	1·24	1·20
Artificial earthquake in Group 1 (Figure 6(f))–AR6(f)			
RGEB/AR6(f)	1·02	1·04	1·29
ARGEB(G1)/AR6(f)	0·61	0·74	1·80
ARGEB(G4)/AR6(f)	0·78	0·91	1·93
Artificial earthquake in Group 2 (Figure 7(b))-AR7(b)			
RGEB/AR7(b)	1·07	0·99	1·41
ARGEB(G1)/AR7(b)	1·12	1·29	1·76
ARGEB(G4)/AR7(b)	0·95	1·08	1·75
Artificial earthquake in Group 2 (Figure 7(d))-AR7(d)			
RGEB/AR7(d)	0·90	1·07	1·32
ARGEB(G2)/AR7(d)	1·44	1·11	1·25
ARGEB(G4)/AR7(d)	1·22	0·93	1·23
Artificial earthquake in Group 3 (Figure 8(b))-AR8(b)			
RGEB/AR8(b)	1·00	1·13	1·45
ARGEB(G3)/AR8(b)	0·97	1·10	1·74
ARGEB(G4)/AR8(b)	0·85	1·74	1·60
Artificial earthquake in Group 3 (Figure 8(g))-AR8(g)			
RGEB/AR8(g)	0·99	0·94	1·21
ARGEB(G3)/AR8(g)	1·12	0·98	1·14
ARGEB(G4)/AR8(g)	0·99	0·90	1·04

acceptable prediction of the maximum response for unknown earthquakes of a given global energy bound. The reduction factor remains constant for different levels of the energy-bound.

It has been found that the average reduction factor is sensitive to the location of the records that defines the subset from which it was determined. In addition, it was found that the average reduction factor for records in a subset with the same general location is not sensitive to time. Thus, for a certain location if sufficient records of previous earthquakes are available, regardless of the chronology of the event, the average reduction factor can be determined with some confidence. An alternative procedure is to determine the average reduction factor from site-specific spectra whenever they are available.

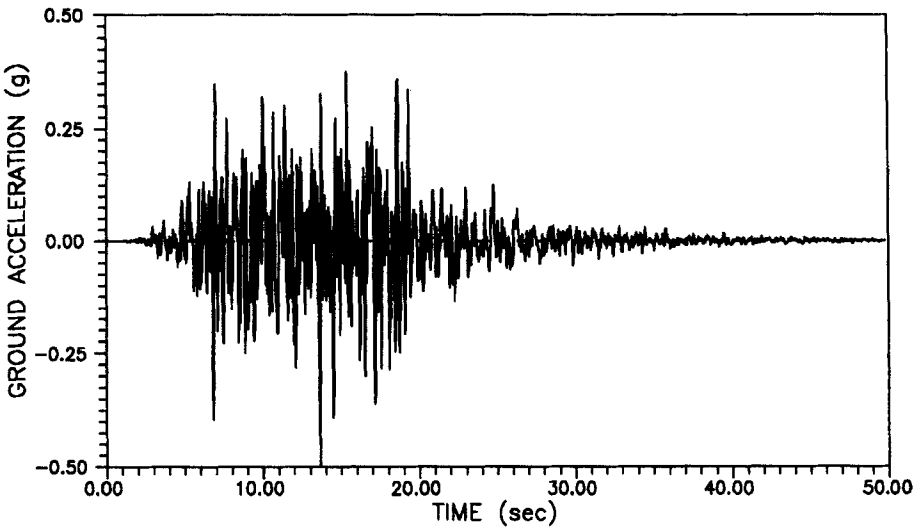

Figure 9. Artificial earthquake using the spectrum of Figure 7(a)

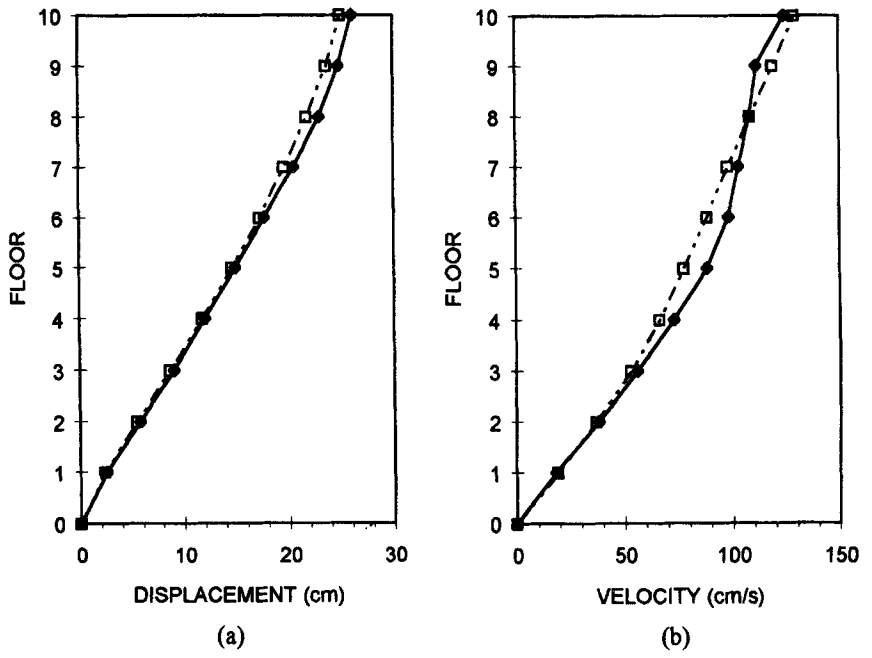

Figure 10. Comparison of the predicted response with the actual record (a) displacement and (b) velocity; (—●—) actual record (AR); (---⊟---) estimated results obtained by the ARGEB convex model of artificial earthquakes in Group 2

ACKNOWLEDGMENTS

Financial support by the National Science Foundation under Grant No. MSS-9207252 is gratefully acknowledged. The authors would like to thank the reviewers for their comments.

APPENDIX

The expressions for velocity and acceleration response of the ith normal mode are given in what follows. Note that the expression for velocity is necessary for evaluation of the control forces in the case of an actively controlled structure.[22] The expression for the acceleration is given for completeness, and for cases where the actively controlled structure will be designed for comfort rather than for safety; in the case of designing for comfort, acceleration constraints are required.[26] Differentiating equation (2) yields for the ith mode velocity

$$\dot{y}_i(t) = e^{-\xi_i\omega_i t}\left\{\int_0^t \phi_i^T \Theta \ddot{X}_g(\tau) e^{\xi_i\omega_i\tau}\cos\omega_{D,i}(t-\tau)\,d\tau - \frac{\xi_i}{\zeta_i}\int_0^t \phi_i^T\Theta\ddot{X}_g(\tau)e^{\xi_i\omega_i\tau}\sin\omega_{D,i}(t-\tau)\,d\tau\right\} \tag{7}$$

Similarly, for the ith mode acceleration differentiating equation (7) yields

$$\ddot{y}_i(t) = \phi_i^T\Theta\ddot{X}_g(t) - 2\xi_i\omega_i e^{-\xi_i\omega_i t}\int_0^t \phi_i^T\Theta\ddot{X}_g(\tau)e^{\xi_i\omega_i\tau}\cos\omega_{D,i}(t-\tau)\,d\tau$$
$$+\left[\frac{(\xi_i\omega_i)^2}{\omega_{D,i}} - \omega_{D,i}\right]e^{-\xi_i\omega_i t}\int_0^t \phi_i^T\Theta\ddot{X}_g(\tau)e^{\xi_i\omega_i\tau}\sin\omega_{D,i}(t-\tau)\,d\tau \tag{8}$$

The peak values of displacement, velocity and acceleration using convex models can be found as follows.[12] For the GEB convex model, the set of admissible ground accelerations was given in equation (4); the maximum displacement can be obtained using equation (2) for the ith normal mode as

$$y_{GEB,i}(t) = \max_{\ddot{X}_g(t)\in S_{GEB}}\left\{\frac{\phi_i^T\Theta}{\omega_{D,i}}\int_0^t \ddot{X}_g(t)e^{-\xi_i\omega_i(t-\tau)}\sin\omega_{D,i}(t-\tau)\,d\tau\right\} \tag{9}$$

Since $y_{GEB,i}(t)$ is a linear function of the ground acceleration, which is assumed to belong to the convex set of equation (4), the maximum in equation (9) occurs on the set of extreme points of the set S_{GEB}.[12] According to the Cauchy–Schwarz inequality[27] for arbitrary functions $f_1(t)$ and $f_2(t)$

$$\left(\int_0^t f_1(\tau)\,f_2(\tau)\,d\tau\right)^2 \leqslant \left(\int_0^t f_1^2(\tau)\,d\tau\right)\left(\int_0^t f_2^2(\tau)\,d\tau\right) \tag{10}$$

with equality occurring only if $f_1(\tau)$ and $f_2(\tau)$ are proportional. The maximizing profile on the interval $[0, t]$ is from equation (9),

$$f_1(\tau) = e^{-\xi_i\omega_i(t-\tau)}\sin\omega_{D,i}(t-\tau) \tag{11}$$

$$f_2(\tau) = \ddot{X}_g(\tau) \tag{12}$$

and for equality in equation (10),

$$\ddot{X}_g(\tau) = \kappa e^{-\xi_i\omega_i(t-\tau)}\sin\omega_{D,i}(t-\tau) \tag{13}$$

The constant κ is determined by substituting equation (13) in equation (9) with a strict equality sign; when κ is substituted back in equation (9) the peak modal displacement is obtained for the GEB convex model as

$$y_{GEB,i}(t) = \frac{\phi_i^T\Theta E_{GEB}}{2\omega_{D,i}}\sqrt{\frac{\lambda_d}{\xi_i\omega_i}},\quad \lambda_d = \zeta_i^2 - e^{-2\xi_i\omega_i t}\left[1 + \zeta_i\xi_i\sin 2\omega_{D,i}t - (\xi_i)^2\cos 2\omega_{D,i}t\right] \tag{14}$$

In a similar manner, as explained in equations (9)–(14) for the peak displacement, the peak modal velocity can be found from equation (7) as

$$\dot{y}_{GEB,i}(t) = \frac{\phi_i^T\Theta E_{GEB}(t)}{2\omega_{D,i}}\sqrt{\frac{\omega_i\lambda_v}{\xi_i}};$$
$$\lambda_v = \zeta_i^2 - e^{-2\xi_i\omega_i t}\left[1 - \zeta_i\xi_i\sin 2(\gamma_i - \omega_{D,i}t) - (\xi_i)^2\cos 2(\gamma_i - \omega_{D,i}t)\right] \tag{15a}$$

$$\gamma_i = \tan^{-1}\left(\frac{\zeta_i}{\xi_i}\right) \tag{15b}$$

Similarly, the peak modal acceleration for the GEB convex model can be found from equation (8) as

$$\ddot{y}_{\mathrm{GEB},i}(t) = \phi_i^{\mathrm{T}} \Theta \ddot{X}_{\mathrm{g}}(t) - \frac{\phi_i^{\mathrm{T}} \Theta E_{\mathrm{GEB}}(t)}{2\zeta_i} \sqrt{\frac{\omega_i \lambda_{\mathrm{a}}}{\xi_i}} \tag{16a}$$

$$\lambda_{\mathrm{a}} = \zeta_i^2[1 + 4(\xi_i)^2] - \mathrm{e}^{-2\xi_i \omega_i t}\,[1 + \zeta_i \xi_i \sin 2(\delta_i + \omega_{\mathrm{D},i} t) - (\xi_i)^2 \cos 2(\delta_i + \omega_{\mathrm{D},i} t)]$$

$$\delta_i = \tan^{-1}\left(\frac{2\xi_i \zeta_i}{\zeta_i - (\xi_i)^2}\right) \tag{16b}$$

The peak values of the modal response using the GEB convex model as time $t \to \infty$ are given in equation (5).

REFERENCES

1. R. F. Drenick, 'Model-free design of aseismic structures', *J. eng. mech. ASCE* **96**, 483–493 (1970).
2. R. F. Drenick, 'Aseismic design by way of critical excitation', *J eng. mech. ASCE* **99**, 649–667 (1973).
3. M. Shinozuka, 'Maximum structural response to seismic excitations', *J. eng. mech. ASCE* **96**, 729–738 (1970).
4. G. Ahmadi, 'Bounds on earthquake response of structures', *J. eng. mech. ASCE* **112**, 351–369 (1986).
5. M. A. Boit, 'A mechanical analyzer for the prediction of earthquake stresses', *Bull. seism. soc. Am.* **31**, 151–171 (1941).
6. G. W. Housner, 'Behavior of structures during earthquake', *J. eng. mech. div. ASCE* **85**, 109–129 (1959).
7. N. M. Newmark, J. A. Blume and K. K. Kapur, 'Seismic design criteria for nuclear plants', *J. power ASCE* **99**, 287–303 (1973).
8. S. H. Crandall, K. L. Chandiramani and R. G. Cook, 'Some first-passage problems in random vibration', *J. appl. mech. ASME* **33**, 532–538 (1966).
9. E. H. Vanmarcke, 'On the distribution of the first passage time for normal stationary random vibration', *J. appl. mech. ASME* **42**, 215–220 (1972).
10. T. H. Heaton and S. H. Hartzell, 'Earthquake ground motions in the near source region', ATC-35-1, *Proc. ATC-35 seminar on new developments in earthquake ground motion estimation and its implications for engineering design practice*, Applied Technology Council Technical Seminar, Redwood City, CA, 1994, pp. 8-1–8-28.
11. F. Naeim and J. C. Anderson, 'Classification and evaluation of earthquake records for design', *The 1993 NEHRP Professional Fellowship Report*, Earthquake Engineering Research Institute, Oakland, CA, July 1993.
12. Y. Ben-Haim and I. Elishakoff, *Convex Models of Uncertainty in Applied Mechanics*, Elsevier, New York, 1990.
13. I. Elishakoff and Y. Ben-Haim, 'Dynamics of a thin cylindrical shell under impact with limited deterministic information on its initial imperfections', *Struct. safety* **8**, 103–112 (1990).
14. H. E. Lindberg, 'An evaluation of convex modeling for multimode dynamic buckling', *J. appl. mech. ASME* **59**, 929–936 (1992).
15. H. E. Lindberg, 'Convex models for uncertain imperfection control in multimode dynamic buckling', *J. appl. mech. ASME* **59**, 937–945 (1992).
16. I. Elishakoff, P. Elisseeff and S. Glegg, 'Convex modeling of material uncertainty on vibrations of a viscoelastic structure', *AIAA J.* **32**, 843–849 (1994).
17. Y. Ben-Haim, 'Fatigue lifetime with load uncertainty represented by convex model', *J. eng. mech. ASCE* **120**, 445–462 (1994).
18. Y. Ben-Haim, 'A non-probabilistic concept of reliability', *Struct. safety* **14**, 227–245 (1994).
19. Y. Ben-Haim, G. Chen and T. T. Soong, 'Maximum structural response using convex models', *J. eng. mech. ASCE* **122**, 325–333 (1996).
20. I. Elishakoff, 'Essay on uncertainties in elastic and viscoelastic structures: from A. M. Freudenthal's criticisms to modern convex modeling', *Comput. struct.* **56**, 871–895 (1995).
21. A. Der Kiureghian, 'Structural response to stationary excitation', *J. eng. mech. div. ASCE* **106**, 1195–1213 (1980).
22. S-R. Tzan and C. P. Pantelides, 'Convex model for seismic design of structures—Part II: design of conventional and active structures', *Earthquake eng. struct. dyn.* **25**, (1996).
23. S-R. Tzan and C. P. Pantelides, 'Convex models for impulsive response for structures', *J. eng. mech. ASCE*, **122**(6), 521–529 (1996).
24. D. A. Gasparini and E. H. Vanmarcke, 'Simulated earthquake motions compatible with prescribed response spectra', *Research Report R76-4, Order No. 527*, Department of Civil Engineering, Constructed Facilities Division, Massachusetts Institute of Technology, Cambridge, MA, 1976.
25. E. H. Vanmarcke, J. M. Biggs, R. Frank, D. Gasparini, G. Gazetas, P. Arnold and W. Luyties, 'Comparison of seismic analysis procedures for elastic multiple-degree system', *Research Report R76-5, Order No. 528*, Department of Civil Engineering, Constructed Facilities Division, Massachusetts Institute of Technology, Cambridge, MA, 1976.
26. C. P. Pantelides, 'Active control of wind-excited structures', *J. wind eng. ind. aerodyn.* **36**, 189–202 (1990).
27. G. H. Hardy, J. E. Littlewood and G. Pólya, *Inequalities*, Cambridge University Press, Cambridge, 1934.